J. Fluid Mech. (1978), *vol.* 86, *part* 2, *pp.* 225–246
Printed in Great Britain

The instabilities of finite-amplitude barotropic Rossby waves

By RICHARD P. MIED

Ocean Sciences Division, Naval Research Laboratory, Washington, D.C. 20375

(Received 6 December 1976 and in revised form 3 October 1977)

The stability of a plane Rossby wave in a homogeneous fluid is considered. When the two-dimensional equation which governs fluid flow on a beta-plane is linearized in the disturbance stream function, a partial differential equation with a periodic coefficient results. Substitution of a solution dictated by the Floquet theory leads to a determinant equation, and it may be shown from its symmetry properties that disturbances to a Rossby wave may be of only two types: (i) neutrally stable modes not necessarily contiguous to a stability boundary and (ii) a pair of temporally unstable waves, one growing and the other decaying.

The determinant is solved numerically for the neutral-stability boundaries and curves of constant disturbance growth rate; two distinct types of instability emerge. The first is the parametric instability, which renders all waves unstable, and is shown to be asymptotic to the classical nonlinear resonant interaction in the limit of vanishing basic-state amplitude. The details of the disturbance frequency bifurcation for zero-amplitude basic-state waves are presented, and calculations for waves with eastward and westward group velocities are made and discussed in the context of Rhines' (1975) results for waves and turbulence on a beta-plane. In addition, a second type of instability is computed which is separate and distinct from the parametric instability. The very limited evidence presented suggests that this second kind of instability may possess characteristics which are identifiable in part with the shearing of the fluid by the large-amplitude basic state and in part with the overturning of the ambient vorticity gradient.

1. Introduction

The atmosphere and oceans exhibit lateral inhomogeneities whose horizontal extents may be much smaller than the overall boundary dimensions of the respective medium. The sources and behaviour of these mesoscale phenomena have been the object of a great deal of intensive study. Baroclinicity and the influence of bottom topography are of crucial importance in describing the dynamics of these systems; however simplified models which address themselves to even more basic underlying phenomena can yield impressive results. For example, Rhines (1975) has attempted to model barotropic turbulence and waves with a simple beta-plane model which retains only the advective nonlinearity, bottom friction and viscous dissipation; some interesting results have emerged from this study.

As a result of his calculations, he points out that nonlinearities favour the transfer of energy into the motions with longer time and length scales, which is precisely the region of space and time in which the beta effect becomes important. Rhines argues that there exists a limiting size for eddies, which seems to be corroborated by observation, and his work underlines the importance of nonlinearities to Rossby wave motions.

In a somewhat related paper, Firing & Beardsley (1976) have followed the evolution of a barotropic eddy on a beta-plane. Their results indicate that, when the Rossby number is not small, the nonlinear evolution of an eddy is qualitatively different from that observed when the eddy is synthesized from a sum of many Rossby waves and allowed to evolve linearly. The observed differences are presumably due at least in part to the mutual interaction and the concomitant energy interchange among these waves. Longuet-Higgins & Gill (1967) first calculated the details of the interaction and found that nonlinear resonant interactions somewhat similar to the mutual interaction of internal gravity waves take place among Rossby waves.

Also of interest in this context is the work of Lorenz (1972), who, motivated by questions of the predictability of the atmosphere, found that simple barotropic Rossby waves in the presence of a uniform westerly current were unstable, although the precise mechanism was unclear. Later, Hoskins & Hollingsworth (1973) noted the critical dependence of the instability upon the disturbance phase speed. Gill (1974) was the first to observe that for vanishing amplitude, however, a Rossby wave exhibits an instability that is actually a nonlinear resonant interaction, while, for large amplitudes, the instability is caused by the shearing motion of the wave itself. The resonant identity of the small-amplitude instability would appear also to follow from Hasselmann's (1967) general theorem regarding the nature of second-order resonant instabilities. Thus the instability of small-amplitude Rossby waves is of a parametric nature and similar to that observed by Baines (1976) for Rossby–Haurwitz waves and by McEwan & Robinson (1975) and Mied (1976) for internal gravity waves.

In the present work we again examine the parametric instability and the instability of the second kind for finite-amplitude Rossby waves in an inviscid fluid on a beta-plane. This is accomplished essentially by the use of the Floquet theory of Gill (1974), but relies heavily upon the numerical solution of the resulting large Hill's determinant using complex arithmetic. By viewing the interaction problem for an arbitrarily large basic-state amplitude as a parametric instability involving many disturbance modes, it is hoped that the limits of validity of Gill's truncated solution, which considers small-amplitude basic-state waves, may be established and that some salient features of the parametric interaction of a single finite-amplitude wave with infinitesimal waves will become apparent. Another facet of this work, however, deals with some effects which occur at very large basic-state amplitudes. Among these are the occurrence of the instability of the second kind, which appears to require the existence of a critical basic-state amplitude, and the behaviour of the parametric instability for these large wave amplitudes. In particular, we present some very limited numerical evidence which tends to suggest that the two instabilities are separate and distinct.

While this work was being reviewed, several papers have appeared in the literature which are related to the present one. Plumb (1977) has discussed the problem of the stability of small-amplitude Rossby waves in a channel, while Gavrilin & Zhmur (1977) have examined the baroclinic instability of small-amplitude waves. Coaker (1977) has established the relationship of the small-amplitude phase instability with the classical asymptotic case. The principal manner in which these three studies differ from the present one lies fundamentally in the basic-state amplitude ranges treated and in the fact that the instability of the second kind has been briefly discussed in the present work.

2. Rossby waves in a homogeneous fluid

The conservation of vorticity of a fluid column of height H is expressed by

$$\frac{d}{dt}\frac{(\zeta+f)}{H} = 0, \tag{1}$$

where $f = 2\Omega \sin(\text{latitude})$, Ω = earth's rotation frequency, $\zeta = +\nabla^2\Psi$ and Ψ is the stream function. If the $+x$ and $+y$ axes are aligned with the easterly and northerly directions respectively, the stream function is related to the velocity by $\mathbf{u} = (-\Psi_y, \Psi_x)$. For a fluid shell of constant depth, (1) may be written in terms of the stream function Ψ and β, the northward gradient of f:

$$\nabla^2\Psi_t + \beta\Psi_x = \Psi_y\nabla^2\Psi_x - \Psi_x\nabla^2\Psi_y. \tag{2}$$

By neglecting the right-hand side of (2), the linearized problem can be shown to admit the gravity-wave solution

$$\Psi = Uk^{-1}\sin(lx + my + \omega t) \tag{3}$$

provided that

$$\omega = \beta l/k^2, \tag{4}$$

where U is the maximum particle speed, $k = |\mathbf{k}| = (l, m)$ and ω is the frequency.

By virtue of the incompressibility condition $\nabla \cdot \mathbf{u} = 0$, these waves are transverse, their wavenumber being perpendicular to the particle paths. Because of this transverse character of the wave propagation, (3) also satisfies the right-hand side of (2) and is thus an exact nonlinear solution.

Although these waves are exact solutions of the vorticity equation, a sum of two or more of them will not in general satisfy (2) exactly unless certain constraints are placed upon that sum. In particular, Longuet-Higgins & Gill (1967) have shown that second-order nonlinear resonant interactions can take place among three freely propagating Rossby waves provided that their frequencies ω_i and wavenumbers $\mathbf{k}_i$ sum to zero. Thus

$$\omega_1 + \omega_2 + \omega_3 = 0, \quad \mathbf{k}_1 + \mathbf{k}_2 + \mathbf{k}_3 = 0. \tag{5}$$

In figures 1 (*a*) and (*b*),† the locus of waves which are possible candidates for such an interaction with the wave $\mathbf{k}_2$ is shown. Of the waves pictured however, only a significantly smaller portion will actually participate in the resonant depletion of $\mathbf{k}_2$ energy. This additional restriction arises because energy may flow from $\mathbf{k}_2$ only when the wavenumbers are ordered such that

$$|\mathbf{k}_1| < |\mathbf{k}_2| < |\mathbf{k}_3|.$$

Gill (1974) has shown that this restriction is valid even when one of these waves becomes of finite amplitude, and this statement is corroborated by the numerical work presented in §§ 3 and 4.

† In this figure and in all of the work which follows, the disturbance frequencies are taken as positive so that the actual direction of phase propagation is opposite to the wavenumber direction. This is in contrast to the frequency of the basic state, which turns out to be negative, so that its phase propagation is always in the direction shown.

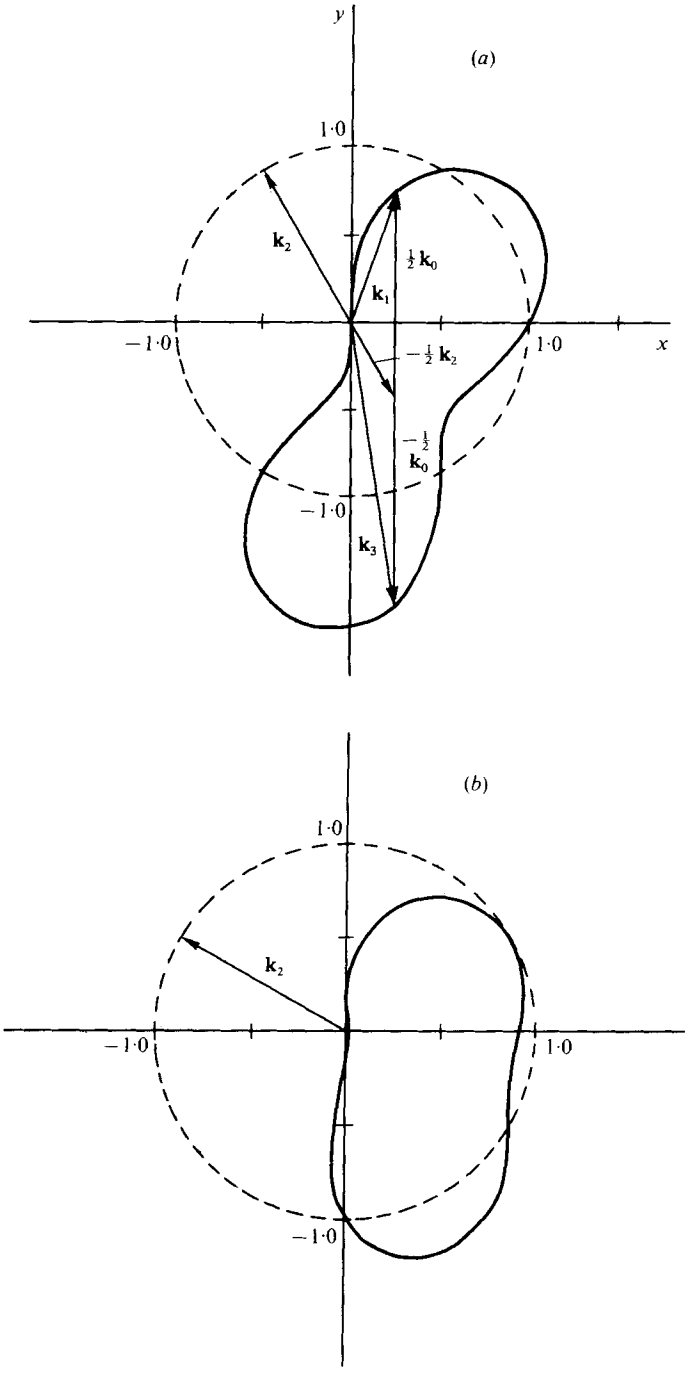

FIGURE 1. (*a*) The closed solid contour represents all waves which satisfy the resonance conditions (5) and the dispersion relation (4). The vector $-\frac{1}{2}\mathbf{k}_2$ extends from the origin to the geometrical centre of the figure, thus $\mathbf{k}_1$, $\mathbf{k}_3 = \frac{1}{2}(-\mathbf{k}_2 \pm \mathbf{k}_0)$. The dashed line represents a kinematical limit (see § 2) such that energy flows from $\mathbf{k}_2$ provided that $|\mathbf{k}_1| < |\mathbf{k}_2| < |\mathbf{k}_3|$. Here $\theta = 120°$ and we normalize $|\mathbf{k}_2|$ as 1. (*b*) The closed contour and dashed circle are as in (*a*) but in this case $\theta = 150{\cdot}0°$; and $|\mathbf{k}_2|$ is again normalized to unity.

3. The parametric instability of barotropic Rossby waves

3.1. *The governing equation*

In § 2, it was mentioned that the Rossby wave given by (3) and (4) is an exact solution of the beta-plane equation (2). This fact affords us the opportunity to examine the consequences of allowing the amplitude of the wave to become quite large and to investigate the parametric instability at these large amplitudes.

Accordingly, let us express the stream function of the flow as a sum of the basic-state wave and a disturbance part, so that

$$\Psi = Uk^{-1}\sin(lx+my+\omega t)+\psi, \tag{6}$$

where $\omega = \bar{\beta}l/k^2$. Substitution of (6) into (2), which governs the conservation of vorticity for the disturbance ψ, gives†

$$\nabla^2\psi_t+\bar{\beta}\psi_x = Uk\cos\phi(m\psi_x-l\psi_y)+Uk^{-1}\cos\phi(m\nabla^2\psi_x-l\nabla^2\psi_y), \tag{7}$$

where $\phi = lx+my+\omega t$ and terms nonlinear in ψ have been neglected. To facilitate comparison with the work of Longuet-Higgins & Gill (1967), the equivalence $\mathbf{k} = \mathbf{k}_2$ is made.

Equation (7) may be non-dimensionalized through the introduction of the quantities

$$(\hat{x},\hat{y}) = k(x,y), \quad \hat{t} = \bar{\beta}k^{-1}t, \quad \hat{\psi} = kU^{-1}\psi.$$

Introducing these variables into (7) and dropping the carets, we have

$$\nabla^2\psi_t+\psi_x = \frac{Uk^2}{\bar{\beta}}\cos\phi\left[\left(\frac{m}{k}\psi_x-\frac{l}{k}\psi_y\right)+\left(\frac{m}{k}\nabla^2\psi_x-\frac{l}{k}\nabla^2\psi_y\right)\right]. \tag{8}$$

Because the phase of the basic-state wave propagates at an angle θ ($90^\circ < \theta < 270^\circ$) to the $+x$ axis considerable simplification of (8) may be gained by introducing a rotated co-ordinate system (ξ, η). From figure 2, we see that

$$\xi = x\sin\theta - y\cos\theta, \quad \eta = x\cos\theta + y\sin\theta$$

and that $l/k = \cos\theta$ and $m/k = \sin\theta$. The governing equation thus becomes

$$\nabla^2\psi_t+(\sin\theta\psi_\xi+\cos\theta\psi_\eta) = M\cos\phi\,(\psi_\xi+\nabla^2\psi_\xi), \tag{9}$$

where $\phi = \eta + t\cos\theta$ and $M = Uk^2/\bar{\beta}$ is a measure of the wave amplitude.

Equation (9) may be seen to possess a separable Floquet solution of the form

$$\psi = \exp[\lambda t+i(\alpha\xi+\beta\eta)]\sum_{n=-\infty}^{+\infty}\psi_n\exp in\phi, \tag{10}$$

where α and β are real, and λ and ψ_n may be considered complex. Substituting (10) into (9) and re-indexing the sums leads to a recursion relation which links three contiguous ψ_n's:

$$\alpha M(q_{n-1}-1)\psi_{n-1}+2i(q_n\lambda_n-p_n)\psi_n+\alpha M(q_{n+1}-1)\psi_{n+1} = 0, \quad n = 0, \pm1, \pm2, \ldots, \tag{11}$$

and

$$\lambda_n = \lambda+in\cos\theta, \quad q_n = (n+\beta)^2+\alpha^2,$$
$$p_n = i[\alpha\sin\theta+(n+\beta)\cos\theta].$$

† Equation (7) corresponds to equation (2.9) of Gill (1974) and his solution (3.8) is equivalent to equation (10) below, except for a rotation of the co-ordinate axes.

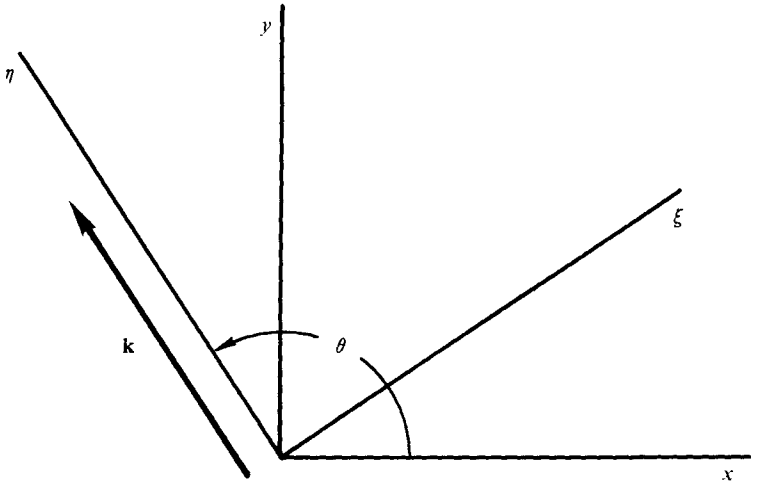

FIGURE 2. The $+x$ axis is directed due east, while the $+y$ axis points north. The ξ, η co-ordinate system is rotated such that the η axis is aligned with the direction θ of phase propagation of the basic-state wave.

Gill (1974) has shown that (11) (his equation 3.13) must contain the essential physics of the classical nonlinear resonant interaction when $U = 0$ (or $M = 0$ here), so that the parametric instability (for $M \neq 0$) must reduce to this well-known case in the asymptotic limit $M \to 0$. By expressing the ψ_n and λ_n as a power series in M, we may formalize this argument.

3.2. *The analytical approach for small M*

Since *a priori* knowledge of the behaviour of the asymptotic limit suggests that two parasitic waves with which the basic state is resonant must dominate the solution, we write

$$\begin{aligned}
\psi_0 &\sim 1 + \psi_{01} M + \ldots, \\
\psi_1 &\sim \psi_{10} + \psi_{11} M + \ldots, \\
\psi_n &\sim O(M), \quad n \neq 0, 1, \\
\lambda &\sim {}_0\lambda + {}_1\lambda M + \ldots,
\end{aligned}$$

where the leading term in ψ_0 has been arbitrarily normalized to unity. Equation (11) reveals the following balances, correct to $O(M)$. For $n = 0$, the $O(M^0)$ and $O(M)$ equations are, respectively,

$$-2(\beta^2+\alpha^2)\,{}_0\lambda + 2i(\alpha\sin\theta + \beta\cos\theta) = 0, \tag{12a}$$

$$+2i(\beta^2+\alpha^2)\,{}_1\lambda + \alpha[(1+\beta)^2+\alpha^2-1]\,\psi_{10} = 0, \tag{12b}$$

while, for $n = 1$, the $O(M^0)$ and $O(M)$ equations are

$$-2[(1+\beta)^2+\alpha^2]\,({}_0\lambda + i\cos\theta) + 2i[\alpha\sin\theta + (1+\beta)\cos\theta] = 0, \tag{13a}$$

$$+\alpha(\beta^2+\alpha^2-1) + 2i[(1+\beta)^2+\alpha^2]\,{}_1\lambda\psi_{10} = 0. \tag{13b}$$

From (12a) we see that $${}_0\lambda = \frac{\alpha\sin\theta + \beta\cos\theta}{\alpha^2+\beta^2}\,i,$$

while (13a) leads to $${}_0\lambda = \left[\frac{\alpha\sin\theta + (1+\beta)\cos\theta}{\alpha^2+(1+\beta)^2} - \cos\theta\right] i.$$

The apparent ambiguity in the value of ${}_0\lambda$ is spurious, and actually serves to define a curve $\beta = \beta(\alpha; \theta)$ along which parametric instabilities for $M \simeq 0$ are possible. To see this we eliminate ${}_0\lambda$ from the above two equations and obtain after some manipulation

$$\beta = \left\{\frac{\alpha \sin\theta + (1+\beta)\cos\theta}{[(1+\beta)^2+\alpha^2]\cos\theta} - 1\right\}(\beta^2+\alpha^2) - \alpha\tan\theta. \tag{14}$$

By fixing α and iterating on β, it may indeed be verified that the resulting curves $\beta = \beta(\alpha; \theta)$ are the resonance loci shown in figures 1 (*a*) and (*b*).

The equations obtained from the $O(M)$ terms [(12*b*) and (13*b*)] are readily solved to yield

$$\psi_{10} = \pm\left\{\frac{(\beta^2+\alpha^2)(\alpha^2+\beta^2-1)}{[(1+\beta)^2+\alpha^2-1][(1+\beta)^2+\alpha^2]}\right\}^{\frac{1}{2}},$$

$${}_1\lambda^2 = -\frac{\alpha^2[\beta^2+\alpha^2-1][(1+\beta)^2+\alpha^2-1]}{4[\beta^2+\alpha^2][(1+\beta)^2+\alpha^2]}.$$

All of the square-bracketed expressions on the right-hand side are positive semi-definite, with the exception of $[\beta^2+\alpha^2-1]$. From (10) we see that $(\alpha^2+\beta^2)^{\frac{1}{2}}$ is the magnitude of the Floquet vector multiplying the infinite sum. As was mentioned in § 2, this vector magnitude must always be less than unity if an instability is to occur. Clearly then, ${}_1\lambda$ is real and the complex frequency may be written as

$$\lambda \sim i\frac{\alpha\sin\theta + \beta\cos\theta}{\beta^2+\alpha^2} \pm \left\{\frac{\alpha^2[1-(\beta^2+\alpha^2)][(1+\beta)^2+\alpha^2-1]}{4[\beta^2+\alpha^2][(1+\beta)^2+\alpha^2]}\right\}^{\frac{1}{2}} M + O(M^2). \tag{15}$$

The time scale for the growth is thus of order M^{-1}, while any correction to the speed of propagation for these disturbances must be of order M^2 or higher. We may not proceed to $O(M^2)$ because this quasi-linear disturbance model neglects products of ψ derivatives, which contain $O(M^2)$ terms. The relation between the parametric instability and the nonlinear resonant interaction† has been formalized, however, and will be further discussed in § 3.4.

For finite M, the wavenumber (α, β) can be expected to be a function of M also, as in the related internal-wave problem (Mied 1976). This information is most easily extracted from the system numerically however, and it is to this task that we next turn our attention.

3.3. *The numerical approach for large M*

In the work which follows, it will be convenient to anticipate that λ is complex and thus write

$$\lambda = \lambda_r + i\lambda_i.$$

Then, if we take the complex conjugate of (11) and reverse the sign of λ_r, it may be easily seen that

$$\psi_n(\alpha, \beta, \lambda_r, \lambda_i, M; \theta) = \psi_n^*(\alpha, \beta, -\lambda_r, \lambda_i, M; \theta). \tag{16}$$

This symmetry property implies that a growing mode ($\lambda_r > 0$) must be associated with a decaying one ($\lambda_r < 0$). Thus it follows immediately that the α, β, λ_i, M, θ parameter space possesses only two types of wave: neutrally stable oscillations

† The asymptotic limit $M \to 0$ corresponds to the weak-interaction limit $U = 0$ in Gill's work.

($\lambda_r = 0$) and temporally unstable Rossby waves ($\lambda_r \neq 0$). We remark in this regard that Lorenz (1972) discovered a neutral mode and a pair of growing and decaying waves in the particular problem which he posed.

A second property may be established and is of great utility. By manipulating (11), it may be seen that

$$\psi_n(\alpha, \beta, \lambda_r, \lambda_i, M; \theta) = \psi_n^*(-\alpha, \beta, \lambda_r, -\lambda_i, M; \pi - \theta). \tag{17}$$

We note that this relates the coefficients ψ_n to those obtained by reflecting the basic-state wave in the $-x$ axis [see figure 2 and (6)]. The implication is that by investigating merely the quadrant $90° < \theta < 180°$ the stability properties of Rossby waves of any amplitude may be regarded as known in the half-plane $90° < \theta < 270°$. The emergence of this property from (11) is not unexpected, and it further serves as a check on the numerical results.

The substitution, in turn, of the integer values $n = 0, \pm 1, \pm 2, \ldots$ into (11) will yield an infinite number of homogeneous equations, although it is hoped that the truncation of the determinant at $n = \pm N$ will converge, before N becomes too large, to the results obtained for the infinite determinant. A sufficient condition for these equations to possess a solution is that the determinant $\Delta(\alpha, \beta, \lambda_r, \lambda_i, M; \theta)$ vanishes. This determinant, which is evaluated by Gaussian elimination (Noble 1969, p. 211), is complex, so that the requirement $\Delta = 0$ in fact imposes two restrictions, namely

$$\operatorname{Re}\Delta = 0, \quad \operatorname{Im}\Delta = 0. \tag{18}$$

It is helpful to point out that the solution of (18) really involves the following question. Given a basic-state wave with direction θ, as well as a disturbance set that grows at a rate λ_r with a particular Floquet vector (α, β), what is the frequency λ_i of that disturbance and what is the basic-state amplitude M required for that growth rate?

The solution of (9) thus relies upon a search for roots in the λ_i, M plane after specifying α, β, λ_r and θ as parameters. This is seen to be the case because the loci of the zeros of the real and imaginary parts of the determinant (18) are curves in the λ_i, M plane. The location of their crossing point(s) in this plane will then specify a complete solution to the problem. Recourse can be had to the method of 'boxing in' the root by successively halving the size of a square in the λ_i, M plane, but the more efficient Newton–Raphson technique is employed in this work (see appendix). The advantage is that one need know only the approximate location of the root and supply this first guess to the iterative scheme in order that the root emerges after several iterations. Although no systematic study has been made of the convergence properties of the method, this iterative technique always seems to converge to a root provided only that the rate of change of Δ with any of its parameters is not excessively large. Some specific comments regarding accuracy and convergence are made in § 4 and in the appendix, however.

3.4. *Discussion of the parametric instability*

From the analytical theory in § 3.2, we can see that the parametric instability is asymptotic in M to the case of the nonlinear resonant instability. In particular, the growth of the instability occurs on time scales of order M^{-1}, while any correction to the frequency λ_i must enter with terms of order M^2 or higher. This would appear to be consistent with the trends observed in other second-order nonlinear resonant theories.

For example, McGoldrick's (1965) calculations of interactions among capillary surface waves and the similar work by Davis & Acrivos (1967) on trapped thermocline waves reveal a similar amplitude-ordering scheme. As the amplitude M of the basic state increases, the instability assumes a parametric character, so that the general result of Hasselmann (1967) is valid also. He observed that nonlinear systems which exhibit an interaction at second order in amplitude will always allow the exponential growth of disturbances at the expense of the basic-state wave provided that the amplitude of that wave is a finite constant.

In the present work, we are interested in finding not only the exponential growth rates, but also the curves in the parameter space which separate neutrally stable Rossby waves from the unstable ones (§ 3.3). Because of the complexity of the physical system (11), the analytical approach can be relied upon to be indicative of trends at small M; however detailed information regarding the nature of the instability is most easily accessible through numerical techniques. With the use of the Newton–Raphson method, detailed information about the roots can be rapidly obtained to arbitrary accuracy (see appendix). These calculations have been performed on an iterative basis until two successive iterations for both roots (λ_i, M) agree to within 0·1 %. While any accuracy is theoretically obtainable, little is gained by proceeding further if the results are to be presented in only graphical form. Although a more thorough discussion of accuracy is given in the appendix, we point out here that all the calculations discussed in this section were performed with a seventh-order determinant ($N_1 = 7$).

In figure 3, the results for a simple neutral-stability curve ($\lambda_r = 0$) and associated curves of constant growth rate are presented. These are plotted in the α, M plane for $\theta = 150°$ and $\beta = -0{\cdot}1$, and appear to be qualitatively similar to those found by Mied (1976) in his investigation of the parametric instability of internal waves. When $M \simeq 0$, i.e. when the basic-state wave has a very small amplitude, the range of the wavenumber α over which instability may occur is vanishingly small. In this neighbourhood of $M = 0$ however, the basic-state and disturbance waves propagate independently of one another, and, concomitantly, this region $M \ll 1$ is the one in which the parametric instability is asymptotic to the nonlinear resonant-interaction formalism. As M is increased however, the range of wavenumbers α which may abstract energy from the basic state is significantly increased. By virtue of the nature of the solution (10), these disturbances are always resonant with the basic state in that wavenumber and frequency constraints similar to the resonance conditions (5) of the asymptotic theory are always valid. The difference lies in the fact that for $M \neq 0$ these disturbance waves must propagate in the presence of a temporally and spatially varying basic state, and this requires that they assume a dispersion relation different from that given by (4) for the case of small-amplitude waves in an otherwise quiescent medium.

It is not generally observed to be the case that all neutral-stability curves in this complicated nonlinear problem qualitatively resemble the V-shape of that in figure 3, or those arising from a similar treatment of the somewhat simpler Mathieu equation (see, for example, Abramowitz & Stegun 1965, chap. 20). In fact, these curves need not necessarily possess the V-shape in the M, wavenumber plane which is assumed in the somewhat limited existing literature as being characteristic of their genre. In figure 4, for instance, the case $\theta = 150°$ is again treated but now β is varied and $\alpha = 0{\cdot}22$. In addition to the odd shape of the $\lambda_r = 0$ curve for moderate values of M, this curve

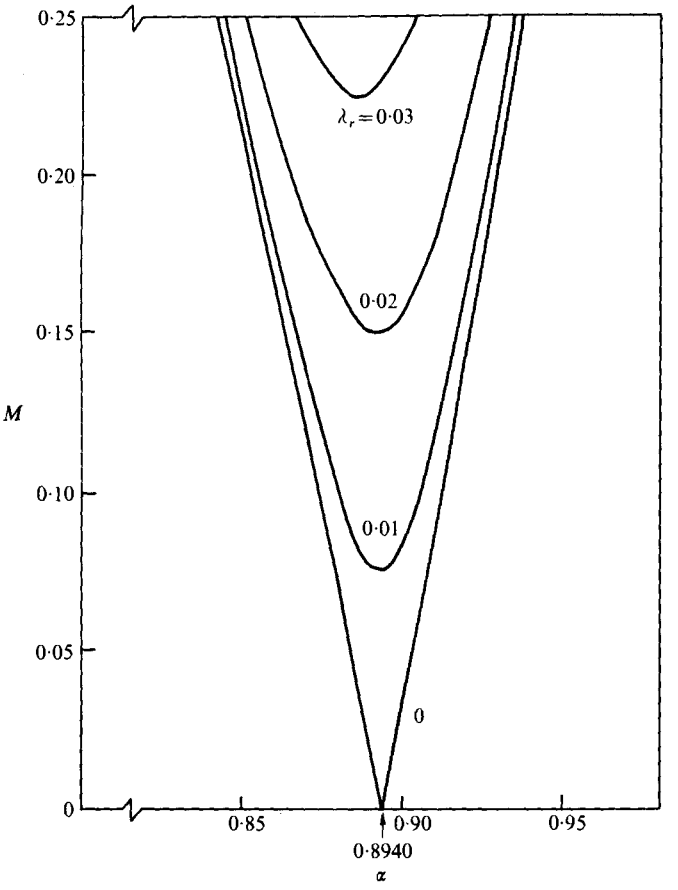

FIGURE 3. The curve of neutral stability $\lambda_r = 0$ and the curves of constant growth rate $\lambda_r = 0{\cdot}01$, $0{\cdot}02$ and $0{\cdot}03$ in the α, M plane. $\theta = 150{\cdot}0°$, $\beta = -0{\cdot}1$ and $N_1 = 7$.

does not continue to broaden with increasingly larger M but instead assumes a vertical slope for some value of $\alpha > 0{\cdot}13$.

Because of the qualitatively dissimilar nature of these two neutral-stability curves, one would suspect that most features of the parametric instability cannot be grasped by conducting somewhat random traverses across the resonance curves pictured in figures 1 (a) and (b). For this reason, it is useful to map the curves of constant M in the α, β Floquet plane when $\lambda_r = 0$. Moreover, the concept of the Floquet plane is a useful one because all the information regarding the instability is contained within the circle $\alpha^2 + \beta^2 \leqslant 1$. This occurs because all Rossby-wave instabilities must include at least one wave whose wavenumber is less than that of the basic state (see § 2). In figure 5, such a plot is made for the case $\theta = 150°$ (with eastward group velocity) and the contours $M = 0$, $0{\cdot}1$, $0{\cdot}2$ and $0{\cdot}3$ are shown; the contour $M = 0$ is, of course, the same resonance curve as is shown in figure 1 (b). The sections AA and BB are those depicted in figures 4 and 3 respectively, while the kinematic limit $\alpha^2 + \beta^2 = 1$ is shown as a dashed line which passes through the end point P at $(0{\cdot}866, -0{\cdot}500)$. All the M = constant curves coalesce at this point. It seems unlikely that this constitutes an ill-defined point because, at least for very small values of M, Longuet-Higgins &

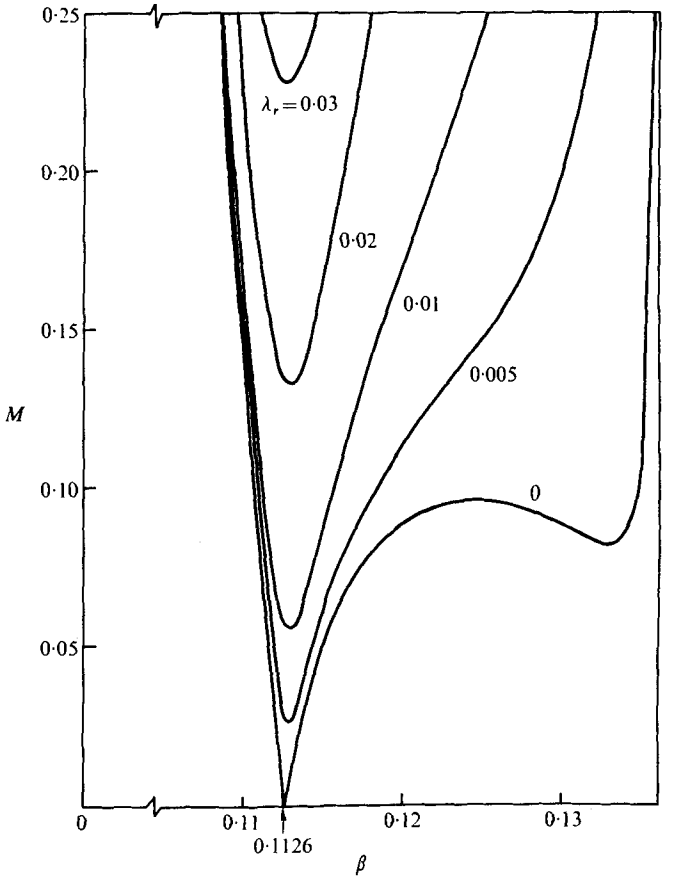

FIGURE 4. The neutral curves $\lambda_r = 0$ and the curves of constant growth rate for $\lambda_r = 0{\cdot}005$, $0{\cdot}01$, $0{\cdot}02$ and $0{\cdot}03$ in the β, M plane. The basic state is propagating at an angle $\theta = 150{\cdot}0°$ to the $+x$ axis, $\alpha = 0{\cdot}22$ and $N_1 = 7$.

Gill (1967) point out that the interaction coefficient which specifies the time rate of change of the wave amplitude vanishes there. A similar phenomenon may be seen in figure 6, which is the Floquet-plane representation for a basic-state wave at $\theta = 120°$ and thus has a westward group velocity. Again, the kinematic limit $\alpha^2 + \beta^2 = 1$ appears as a dashed line and all constant-M contours coalesce at a point on this circular arc.

The Floquet planes for these two test cases, one with an eastward and the other with a westward group velocity, are qualitatively dissimilar. It is interesting to discuss these results in terms of those of Rhines (1975), who observed that, in the case of the temporal evolution of waves and turbulence on a beta-plane, east–west velocities developed at large times; he suggests that these are a steady, quasi-permanent feature of such a system. Although any connexion between the behaviour of an ensemble of waves and the present work may be somewhat tenuous, a discussion of similarities in the present context seems appropriate.

On figures 5 and 6, the direction North is indicated with an arrow and the letter 'N'. When $\theta = 120°$ (westward group velocity), the disturbance waves generated tend to deviate greatly from those arising from the $M = 0$ case. It is apparent, though, that

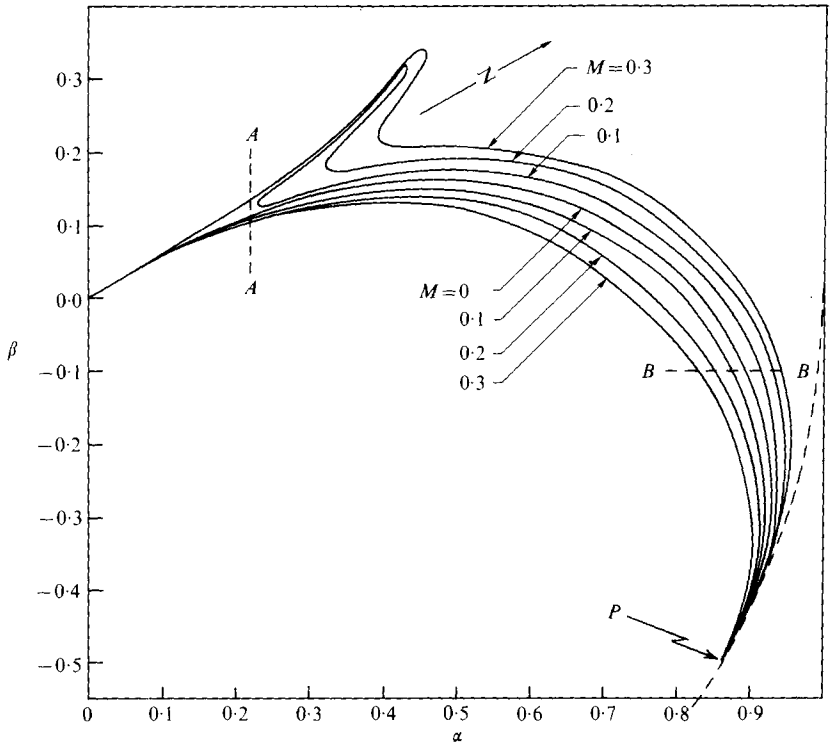

FIGURE 5. The Floquet plane for $\theta = 150°$ and $\lambda_r = 0$. The contours shown are those for basic-state amplitudes $M = 0$ (the resonance curve of figure 1*b*), 0·1, 0·2 and 0·3. The sections AA and BB represent the curves shown in figures 4 and 3 respectively. The dashed line represents the kinematical limit $\alpha^2 + \beta^2 = 1$ and is discussed in § 2.

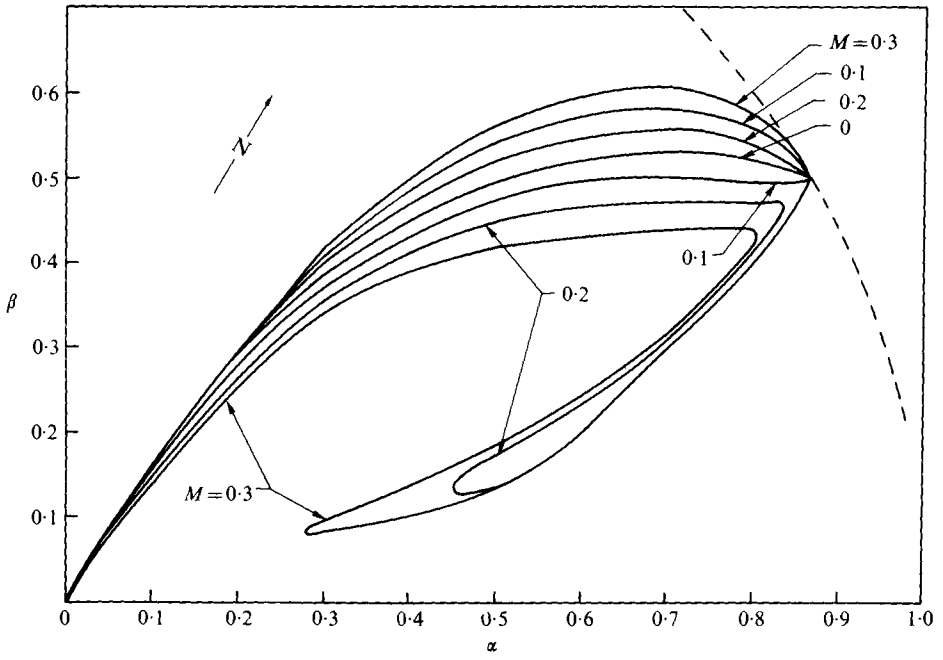

FIGURE 6. The Floquet plane for $\theta = 120°$ and $\lambda_r = 0$. The contours $M = 0$, 0·1, 0·2 and 0·3 are shown. The curve for $M = 0$ is a portion of the resonance locus shown in figure 1 (*a*). These calculations were made for $N_1 = 7$.

the Rossby waves generated possess particle trajectories which are oriented neither north–south nor east–west. On the other hand, examination of the case with eastward group velocity ($\theta = 150°$) indicates that waves of a similar nature are generated, but with one important addition. Referring to figure 5, we see that the barb-like protuberance towards the north (in the vicinity of section AA) clearly indicates that this set of instabilities contains small vertical wavenumbers, and hence very long waves with zonal currents. Of all of the disturbances arising, these southward-propagating waves are perhaps the most temporally permanent feature of the instability, for Longuet-Higgins & Gill (1967) have pointed out that, while such waves may themselves participate in resonant interactions, their role is of a catalytic nature and thus leaves their identity unaltered. *If* these results are generally indicative of those for waves whose groups propagate east and west, we may make the somewhat tenuous conclusion that it is more likely to be the waves which have an eastward group velocity which are at least *one* contributing factor in the appearance of Rhines' zonal currents.

Casual observation of figures 5 and 6 might lead one to the conclusion that the contours of constant basic-state amplitude are not asymptotic to the curve for $M = 0$. This is incorrect, as the neutral-stability curves which generate these lobes are actually of the type shown in figure 4. In no case examined does a trough of the type shown in figure 4 dip down to touch the $M = 0$ axis. Although these results are asymptotic to the zero-amplitude case, they do indicate that finite-amplitude effects are present which may produce results not in direct qualitative agreement with the asymptotic analytic theory.

This linear problem places no constraints upon the amplitudes $|\psi_n|$, with the exception of the stipulation that they be small with respect to that of the basic state. In § 3.2, however, it was shown that, for $M \simeq 0$, ψ_0 and ψ_1 are the largest of the coefficients and possess magnitudes much greater than the others. Figure 7 shows the normalized ratio $|\psi_n/\psi_0|$ for $M \lesssim 0{\cdot}3$ and clearly indicates that $|\psi_{-1}|$ and $|\psi_2|$ are far smaller than either $|\psi_0|$ or $|\psi_1|$; this is especially true for the smaller values of M. The instability thus retains some of its asymptotic (triad) nature for finite M. It is this facet which apparently ensures that the neutral curves calculated with $N_1 = 3$ differ by of the order of only 10 % from those calculated with $N_1 = 7$.

A typical set of dispersion relations associated with the parametric instability is shown in figure 8. Here the frequency λ_i of the $n = 0$ vector (α, β) [see (10)] is plotted as a function of basic-state amplitude M. Curves of constant growth rate $\lambda_r = 0$, 0·02, and 0·03 are shown. At $M = 0$, the value of the frequency λ_i is the same as that given by the linear theory ($_0\lambda$ in § 3.2). At $M = 0$, however, the frequency of the neutrally stable wave bifurcates, so that for $M > 0$ there are two frequencies at which waves can exist for a given value of M. We note also that the wavenumber α can be seen to vary along a curve of constant λ_r, and an interesting phenomenon can be observed from this dispersion plot.

Our assumed flow field consists of a finite-amplitude wave and an infinite sum of infinitesimal-amplitude disturbances. Now consider a field of Rossby waves on a beta-plane. Although not accurate, it is useful for illustrative purposes to consider the finite-amplitude wave as being representative of a typical spectral element in our Rossby-wave ensemble. At time zero, the wave has the amplitude M_1, but after a short time that amplitude has decreased to $M_2 < M_1$, because the parasitic disturbances have gained energy at the expense of the basic state. Referring to figure 8, we see that a

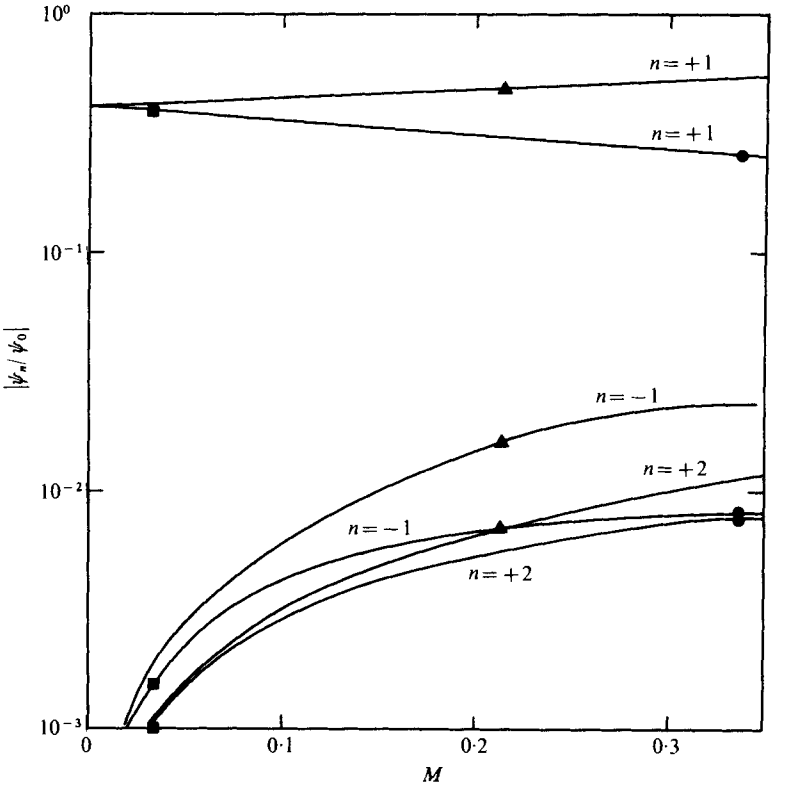

FIGURE 7. $|\psi_n/\psi_0|$ as a function of M for $n = \pm 1$ and 2. $\theta = 150°$, $\lambda_r = 0{\cdot}001$, $N_1 = 7$ and $\beta = -0{\cdot}1$. ▲, $\alpha = 0{\cdot}85$; ■, $\alpha = 0{\cdot}90$; ●, $\alpha = 0{\cdot}95$.

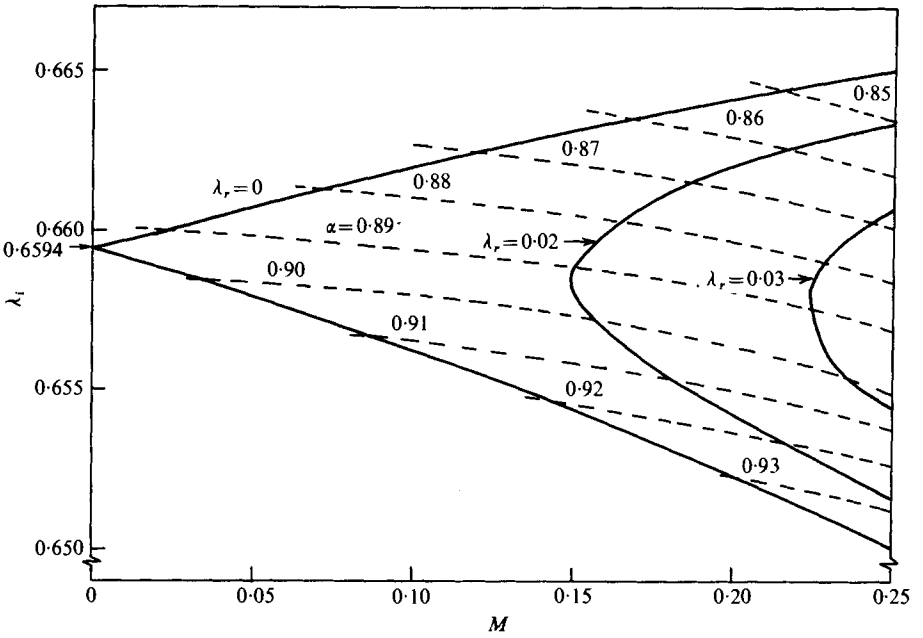

FIGURE 8. The frequency λ_i of the disturbance wave for which $n = 0$ [see (10)] as a function of M. The curves are for growth rates $\lambda_r = 0$, 0·02 and 0·03. In this case $\theta = 150°$, $\beta = -0{\cdot}1$ and $N_1 = 7$. The contours of constant α are shown also.

decrease in M means that our disturbance wave must move to a curve corresponding to a lower growth rate, but which path it takes to do so is open to question. For example, does the disturbance preserve its wavelength by moving along a curve α = constant, or is frequency conserved so that lines of constant wavenumber are crossed? There seems to be no *a priori* reason to believe that a disturbance must conserve its frequency rather than its wavelength or vice versa. Even if it were possible to follow a single wave in a strongly nonlinear evolving system such as this, the character of that wave would change continually. This result serves as a reminder that the concept of a dispersion relation for a member of an ensemble is useful only when the waves are of infinitesimal amplitude and therefore evolve slowly.

4. Instabilities of waves of very large amplitude

Gill (1974) has pointed out that the Rossby-wave instability is of a resonant-interaction nature for $M \ll 1$, while it assumes the character of a shearing instability for $M \gg 1$. For intermediate values of M, one might assume that the two instabilities are the same. This view would be incorrect, as numerical evaluation of the neutral-stability curves indicates that for $M = O(1)$ two separate and distinct instabilities can coexist. Let us briefly examine the behaviour of each type of instability.

In figure 9, a parametric neutral-stability curve ($\lambda_r = 0$) and a curve of constant growth rate ($\lambda_r = 0{\cdot}1$) are shown in their entirety. In this plot, the basic-state amplitude M is shown as a function of the in-line wavenumber β for $\alpha = 0{\cdot}5$ and a direction of travel $\theta = 150°$. For $M \lesssim 0{\cdot}3$, we see that the neutral curve assumes the V-shape so characteristic of the small-amplitude parametric instability. For somewhat larger M however, we immediately perceive the most prominent feature of this neutral-stability curve: that it does not extend upwards indefinitely, but ends in two cusped regions. Thus for sufficiently large amplitudes, no wave is neutrally stable in the parametric sense.

The neutral-stability curve is periodic in β and the reason for this behaviour is clear upon examination of the disturbance solution. From (10) we see that this part of the stream function is given by

$$\psi = \exp[\lambda t + i(\alpha\xi + \beta\eta)] \sum_{-\infty}^{+\infty} \psi_n \exp in(\eta + t\cos\theta).$$

By increasing n by ± 1 and β by ∓ 1, we see that the essential nature of the solution is unchanged provided only that we accept a redefinition of λ. In effect then, the neutral-stability and growth curves have unit period in β, and this character is indicated by the dashed lines on the extreme left and right of figure 9. While the behaviour of λ_i cannot be considered strictly periodic, it is repetitive after a fashion, and the $\lambda_i = \lambda_i(\beta)$ curve associated with the neutral-stability curve of figure 9 is shown in figure 10.

In the previous paragraphs we have noted the behaviour of the parametric instability for moderate M. There exists, however, an instability of the second kind which is operative for somewhat larger values of M; this is shown in figure 11 for the parameter values $\lambda_r = 0$ and $0{\cdot}1$ with $N_1 = 15$, $\alpha = 0{\cdot}5$ and $\theta = 150°$. Here M is shown as a function of β over the same range as in figure 9. Again the stability curves have unit period in β, but it is also interesting to speculate that they might extend to infinity in M. The neutral curves have been calculated for $M \leqslant 12$ and the two upward branches in the centre of the plot show no tendency to coalesce.

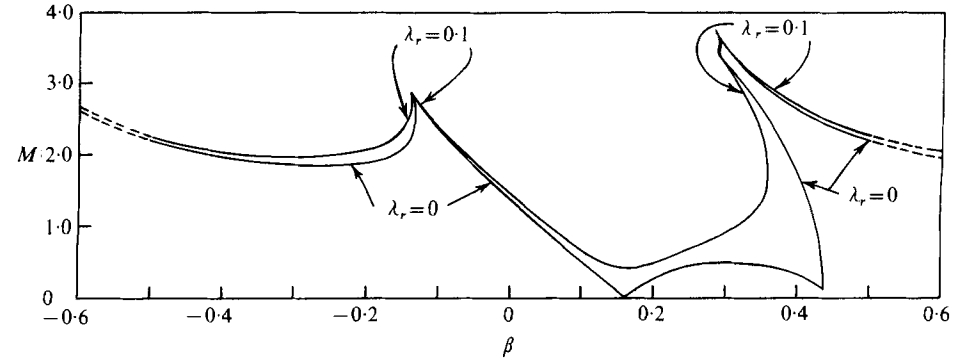

FIGURE 9. The complete neutral-stability curve $\lambda_r = 0$ and the curve of constant growth rate $\lambda_r = 0{\cdot}1$ for the parametric instability. A large determinant ($N_1 = 15$) is required for this case ($\theta = 150°, \alpha = 0{\cdot}5$) and the periodic nature of the curves is indicated by the dashed lines.

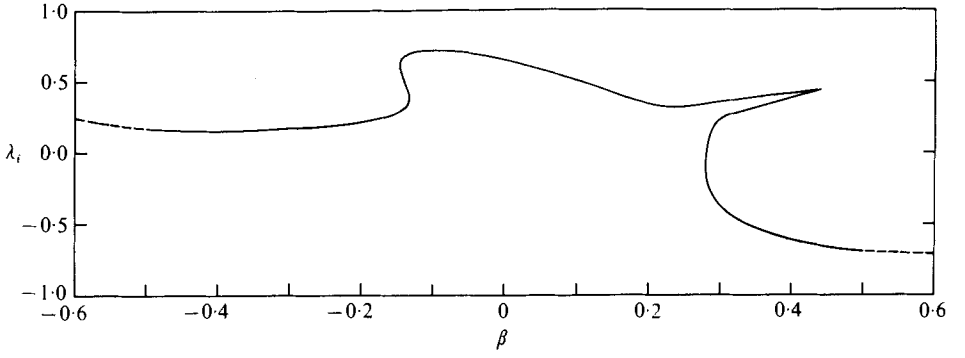

FIGURE 10. The dispersion relation $\lambda_i = \lambda_i(\beta)$ for the $\lambda_r = 0$ curve of figure 10. Here again $N_1 = 15$, $\theta = 150°$ and $\alpha = 0{\cdot}5$.

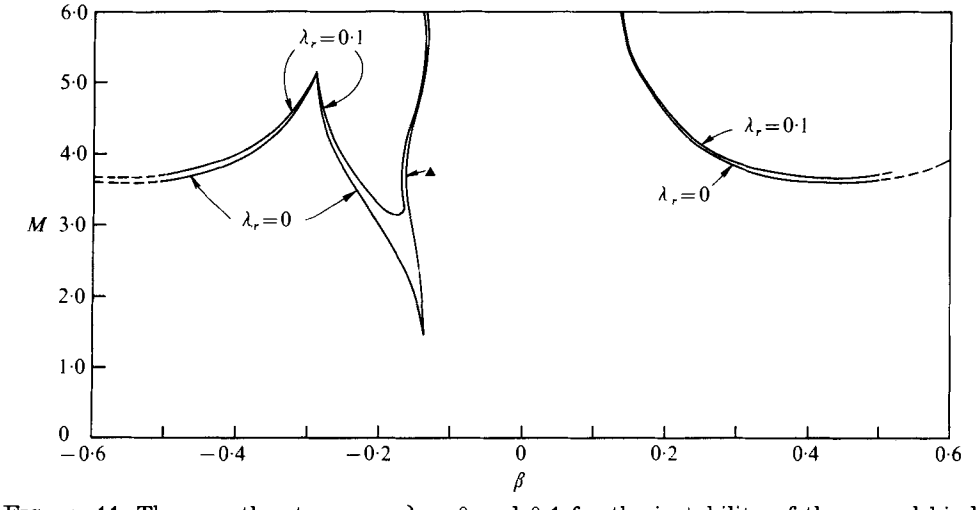

FIGURE 11. The growth-rate curves $\lambda_r = 0$ and $0{\cdot}1$ for the instability of the second kind. The parameter values $N_1 = 15$, $\theta = 150°$ and $\alpha = 0{\cdot}5$ are the same as those for figure 9. The local minimum on the right-hand part of the graph does not correspond to a rotor instability. The triangle at $\beta \simeq -0{\cdot}15$ corresponds to the dispersion relation shown in figure 12.

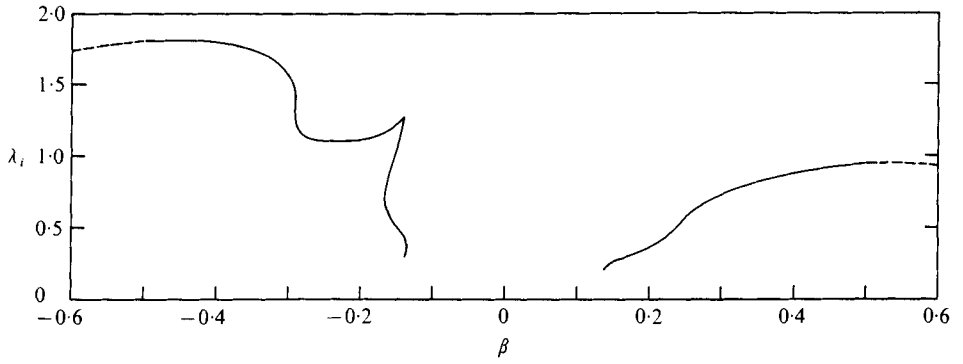

FIGURE 12. The dispersion relation for the instability of the second kind when $\lambda_r = 0$, $N_1 = 15$ and $\alpha = 0{\cdot}5$. The last point on the segment of the curve at $\beta \simeq -0{\cdot}15$ is indicated by the triangle in figure 11. Note the complete lack of similarity of this dispersion relation to that shown in figure 10 for the parametric instability.

Gill (1974) has observed that large-amplitude waves become unstable through the mechanism of shear, but, by analogy with the propagation of plane internal gravity waves, we suspect that a wave of sufficiently large amplitude could also overturn the ambient vorticity structure. A sufficient condition for this overturning instability not to occur is seen to be

$$|\text{maximum horizontal fluid velocity}| < |\text{horizontal phase speed}|.$$

If $\Psi = U/k \sin(lx + my + \omega t)$ and $\omega = \bar{\beta} l/k^2$, then the horizontal fluid velocity is seen to be $-\Psi_y = -(Um/k)\cos(lx + my + \omega t)$ while the horizontal phase speed is ω/l. Recalling that $M = Uk^2/\bar{\beta}$, a sufficient condition for overturning of the ambient vorticity gradient *not* to occur is seen to be

$$M < |1/\sin\theta|.$$

Thus for $\theta = 150°$ the rotor instability might occur for any $M > 2$. Motivated by this simple calculation, we are led to inquire whether the local minimum forming the right-hand part of the stability curve of figure 11 might not be due to this mode of instability. Calculations of this sort for different α have been made, however, and this trough has been observed to fall below $M = 2$ when these different α's are used. While the numerical searches have failed to turn up a stability curve lying wholly above $M = 2$, this limited evidence does not preclude the existence of an overturning instability. What does appear more likely at this point is that the instability of the second kind shown in figure 11 is a mixed shearing and rotor instability for most values of M over which it occurs. For the sake of completeness, and to emphasize the distinctness of the instabilities shown in figures 9 and 11, we include the $\lambda_i = \lambda_i(\beta)$ curve associated with figure 11 in figure 12. While this curve is not remarkable in itself, we do point out that its behaviour is separate and distinct from that of the dispersion relation for the parametric instability shown in figure 10; moreover, the repetitive nature of λ_i is again apparent in this figure.

5. Conclusions and critique

Numerical calculations of the parametric instability of barotropic Rossby waves on a beta-plane in fluid of constant depth have been made. This linearized study has made the approximation that for small times the amplitude of the basic-state wave is a constant, so that technically this work addresses only the question of the *initial tendency* of a disturbance to grow at a certain rate; the emergence of symmetry properties permits results for waves in the quadrant $90° < \theta < 180°$ to be extended to the half-plane $90° < \theta < 270°$.

All such waves are parametrically unstable and for small wave amplitudes this instability reduces to the nonlinear resonant-interaction formalism of Longuet-Higgins & Gill (1967). Moreover, Gill's (1974) kinematic limit, that one disturbance wave must always be longer than the basic-state wave, is corroborated by the numerical work presented in § 3.4. Disturbances to Rossby waves of any amplitude can be of only two types: neutrally stable waves, which are in general not contiguous to a stability boundary, and unstable waves consisting of a temporally growing and decaying pair of the same wavelength, frequency and direction. Examination of the results for the stability of a wave with an eastward group velocity indicates that these instabilities may be one important element in the establishment of the quasi-permanent zonal currents noted by Rhines (1975).

The reader should be cautioned at this point that this rigid-lid theory neglects the levelling effect associated with a free-surface model, so that results for the region $0 \sim (\alpha^2+\beta^2)^{-\frac{1}{2}} \ll L_R$ (the Rossby radius of deformation) may be qualitatively incorrect, even for the barotropic ocean treated in this case.

Because the results of § 3.4 suggest that the rate of energy abstraction from a finite-amplitude Rossby wave can be significant, the calculation of decay times for these waves would be very instructive. This would, however, involve a numerical integration over the area bounded by one of the contours of constant M shown in figures 5 and 6. The rapid variation of this surface $M(\alpha, \beta)$ for slight changes in the dependent variables in some regions of α and β, however, indicates that this calculation would constitute an imposing task indeed.

In § 4, some calculations have been presented which suggest that the parametric instability and that of the second kind may be separate and distinct. In addition, no evidence has been found to point to the existence of a pure overturning instability. While these limited results are interesting in their own right, they represent far too small a subset from which to generalize, and any generalizations made from them must be regarded as wholly conjectural. Nevertheless, it would appear from figures 10 and 12 that the parametric instability is far more important than the second kind in determining the mesoscale dynamics of the oceans. We suspect this because the former instability can exist and grow at a rather *vigorous* rate for basic-state amplitudes insufficiently large even to trigger the growth of the latter type.

Appendix

The matrix of coefficients ψ_n of the recursion relation

$$\alpha M(q_{n-1}-1)\psi_{n-1}+2i(q_n\lambda_n-p_n)\psi_n+\alpha M(q_{n+1}-1)\psi_{n+1}=0,$$
$$n=0,\pm1,\pm2,\ldots,\pm N,$$

where
$$\lambda_n=\lambda_r+i(\lambda_i+n\cos\theta),\quad q_n=(n+\beta)^2+\alpha^2,$$
$$p_n=i[\alpha\sin\theta+(n+\beta)\cos\theta],$$

is tridiagonal and of dimensions $(2N+1)\times(2N+1)$. A sufficient condition for a solution to exist is that the associated determinant $\Delta(\alpha,\beta,\lambda_r,\lambda_i,M;\theta)$ vanishes. If we treat α, β, λ_r and θ as given parameters, we need locate only the crossing point(s) of the two curves

$$\mathrm{Re}\,\Delta\equiv\Delta_r=0,\quad \mathrm{Im}\,\Delta\equiv\Delta_i=0 \tag{A 1}$$

in the λ_i, M plane.

A particularly efficient way to accomplish this is the iterative Newton–Raphson technique (see, for example, Carnahan, Luther & Wilkes 1969, p. 319). Although this method is most widely used to find the roots of an equation with one independent variable, extension to multiple dimensions is quite easy. For convenience, we omit the variables specified as parameters and use only λ_i and M as independent variables.

Suppose that we are close to a root in the λ_i, M plane, but that the actual location of the root is $(\lambda_i+\delta\lambda_i, M+\delta M)$. Then we note that (A 1) will be satisfied identically at the latter point:

$$0=\Delta_r(\lambda_i+\delta\lambda_i, M+\delta M),\quad 0=\Delta_i(\lambda_i+\delta\lambda_i, M+\delta M). \tag{A 2}$$

By expanding the expressions in (A 2) about our estimated root (λ_i, M), we may relate our first guess of the root location to its actual position. That is,

$$\left.\begin{aligned}0=\Delta_r(\lambda_i+\delta\lambda_i,M+\delta M)&=\Delta_r(\lambda_i,M)+\frac{\partial\Delta_r}{\partial\lambda_i}\bigg|_0\delta\lambda_i+\frac{\partial\Delta_r}{\partial M}\bigg|_0\delta M+\ldots,\\ 0=\Delta_i(\lambda_i+\delta\lambda_i,M+\delta M)&=\Delta_i(\lambda_i,M)+\frac{\partial\Delta_i}{\partial\lambda_i}\bigg|_0\delta\lambda_i+\frac{\partial\Delta_i}{\partial M}\bigg|_0\delta M+\ldots,\end{aligned}\right\} \tag{A 3}$$

where the subscript 0 refers to the point (λ_i, M). The calculation of these determinant derivatives is straightforward. Suppose that we define $\boldsymbol{\psi}=(\ldots,\psi_{-1},\psi_0,\psi_1,\ldots)$ so that the system to be solved is of the form $\mathbf{R}.\boldsymbol{\psi}=0$ and thus $\Delta=\det\mathbf{R}=\|\mathbf{R}\|$, say. Then

$$\frac{d}{da}\|\mathbf{R}\|=\sum_{n=-N}^{+N}\|\mathbf{B}\|,$$

where
$$B_{kj}=\begin{cases}R_{kj}, & k\neq n,\\ \partial R_{kj}/\partial a, & k=n,\end{cases}$$

and $a=\lambda_i$ or M. Specifically, the derivatives of the rows are

$$\partial R_{kj}/\partial\lambda_i=(\ldots,0,-2q_n,0,\ldots),$$
$$\partial R_{kj}/\partial M=[\ldots,\alpha(q_{n-1}-1),0,\alpha(q_{n+1}-1),\ldots].$$

Determinant size (N_1)	M	λ_i
3	0·245	0·3697
5	0·23094	0·36729
7	0·230864	0·3672781
9	0·230869	0·3672782
11	0·230876	0·3672783

TABLE 1. Roots obtained by increasing determinant size and observing convergence to the correct value. The difference between values of M calculated with $N_1 = 3$ and $N_1 = 7$ never exceeds of the order of 10 % as long as $M \lesssim 0{\cdot}3$, and accuracy is not materially improved beyond $N_1 = 7$. $\alpha = 0{\cdot}595$, $\beta = 0{\cdot}57$, $\theta = 120°$ and $\lambda_r = 0{\cdot}02$.

M	λ_i	δM	$\delta\lambda_i$
0·155	0·250	1·6552	0·0663
1·810	0·316	−1·3483	−0·0028
0·462	0·313	−0·1433	−0·0085
0·319	0·305	−0·0522	−0·00005
0·266	0·305	−0·0040	0·00000
0·262	0·305	−0·00005	0·00000

TABLE 2. Convergence table for an initial guess of $M = 0{\cdot}155$, $\lambda_i = 0{\cdot}250$. The parameter values are $N_1 = 7$, $\theta = 150°$, $\alpha = 0{\cdot}3724$, $\beta = 0{\cdot}215$ and $\lambda_r = 0{\cdot}001$.

By solving (A 3) for $\delta\lambda_i$ and δM, we obtain explicit values by which we were in error. Thus

$$\delta\lambda_i = [(\partial\Delta_r/\partial M)\Delta_i - (\partial\Delta_i/\partial M)\Delta_r]/D$$

and

$$\delta M = [(\partial\Delta_i/\partial\lambda_i)\Delta_r - (\partial\Delta_r/\partial\lambda_i)\Delta_i]/D,$$

where

$$D = \frac{\partial\Delta_r}{\partial\lambda_i}\frac{\partial\Delta_i}{\partial M} - \frac{\partial\Delta_r}{\partial M}\frac{\partial\Delta_i}{\partial\lambda_i}.$$

These values for $\delta\lambda_i$ and δM are corrections which are added to the initial estimates of λ_i and M. By inserting these updated values into (A 3) an improved estimate can be obtained.

Although successive iterations will refine the knowledge of a given root location, one is necessarily restricted to the limits of accuracy obtainable in the numerical problem *as posed*. Clearly then, a far more serious concern is determinant size. If n successively assumes the values $0, \pm 1, \pm 2, \ldots, \pm N$, the determinant size is given by $N_1 = 2N + 1$, and we expect that increasing N_1 will make the roots converge to a limit. This is in fact the case; indeed, reference to table 1 indicates that this convergence appears to be quite rapid. In table 1, the same set of iterations has been performed repeatedly for $\theta = 120°$ and $\lambda_r = 0{\cdot}02$, but the value of N_1 has been increased by two for each successive root search. As N_1 is increased from 3 to 7, the roots (λ_i, M) never change position by more than about 10 % (for $M \lesssim 0{\cdot}3$), most of the change occurring between $N_1 = 3$ and 5. For $N_1 = 11$ however, the results are always in agreement with those for $N_1 = 7$ to within better than 10^{-5}, again for $M \lesssim 0{\cdot}3$. Evidently, an accuracy criterion that terminates iterations when successive roots agree to within 0·1 % is not restrictive, as after only a few iterations the process converges so rapidly as easily

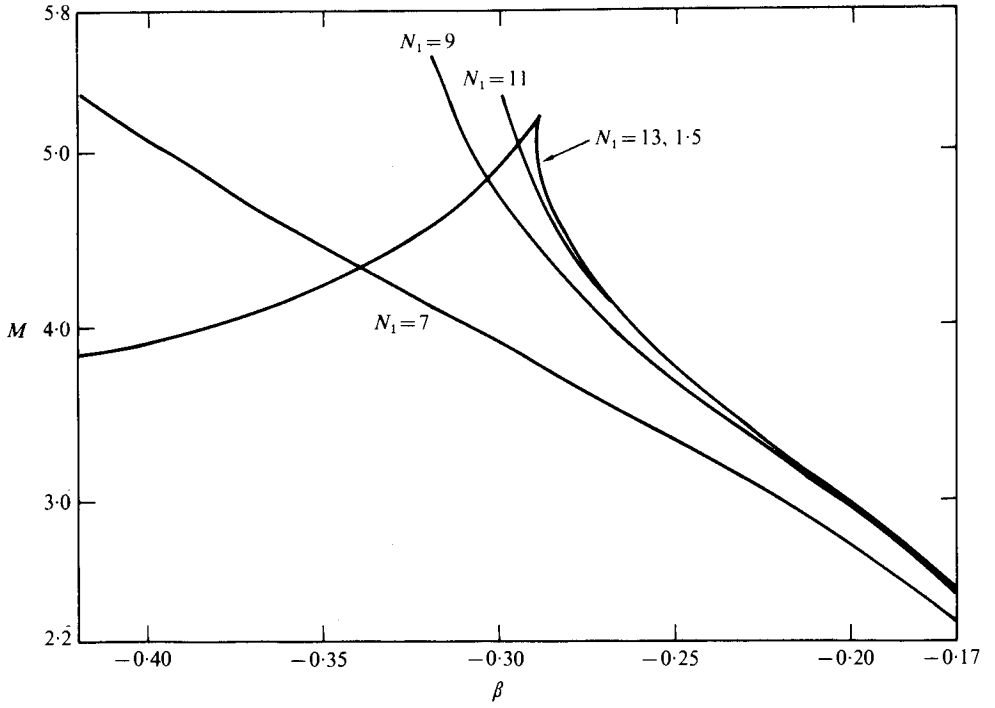

FIGURE 13. Evaluation of the neutral-stability boundary of figure 11 for $N_1 = 7, 9, 11, 13$ and 15. Note that a determinant of relatively high order is required for these very large values of M.

to exceed our expectation of the error. Therefore, since all calculations for the small-amplitude parametric instability have been performed with $N_1 = 7$, we expect that the *de facto* accuracy of these results far exceeds the stated figure of 0·1 %.

It would be incorrect, however, to imply that the choice of determinant size $N_1 = 7$ will always yield correct results when M is of arbitrary size. The Newton–Raphson technique is applied by searching for a root in the λ_i, M plane after first fixing α, β, λ_r and θ. After the root has been obtained, one of the fixed parameters (β, say) is increased by a small amount and the previously found root is used as a starting point for a new iteration. This approach works well in most cases but can lead to problems if the curve loops back on itself or ends in a cusp. In addition to keeping track of the root, care must be taken because it frequently happens that the determinant size required for accuracy in these cases is quite large. In figure 13 for instance, the calculation of a neutral curve (see figure 11 for the complete curve) is performed for $N_1 = 7$, 9, 11, 13 and 15 and we see that in these critical regions we cannot perform calculations with a determinant smaller than of thirteenth or fifteenth order.

REFERENCES

ABRAMOWITZ, M. & STEGUN, I. A. 1965 *Handbook of Mathematical Functions*. Dover.

BAINES, P. G. 1976 The stability of planetary waves on a sphere. *J. Fluid Mech.* **73**, 193.

CARNAHAN, B., LUTHER, H. A. & WILKES, J. O. 1969 *Applied Numerical Methods*. Wiley.

COAKER, S. A. 1977 The stability of a Rossby wave. *Geophys. Astrophys. Fluid Dyn.* **9**, 1.

DAVIS, R. E. & ACRIVOS, A. 1967 The stability of oscillatory internal waves. *J. Fluid Mech.* **30**, 723.

FIRING, E. & BEARDSLEY, R. C. 1976 The behavior of a barotropic eddy on a β-plane. *J. Phys. Ocean.* **6**, 57.

GAVRILIN, B. L. & ZHMUR, V. V. 1977 Stability of Rossby waves in a baroclinic ocean. *Oceanology* **16**, 330.

GILL, A. E. 1974 The stability of planetary waves on an infinite beta-plane. *Geophys. Fluid Dyn.* **6**, 29.

HASSELMANN, K. 1967 A criterion for nonlinear wave stability. *J. Fluid Mech.* **30**, 737.

HOSKINS, B. J. & HOLLINGSWORTH, A. 1973 On the simplest example of the barotropic instability of Rossby wave motion. *J. Atmos. Sci.* **30**, 150.

LORENZ, E. N. 1972 Barotropic instability of Rossby wave motion. *J. Atmos. Sci.* **29**, 258.

LONGUET-HIGGINS, M. S. & GILL, A. E. 1967 Resonant interactions between planetary waves. *Proc. Roy. Soc.* A **299**, 120.

MCEWAN, A. D. & ROBINSON, R. M. 1975 Parametric instability of internal gravity waves. *J. Fluid Mech.* **67**, 667.

MCGOLDRICK, L. F. 1965 Resonant interactions among capillary-gravity waves. *J. Fluid Mech.* **21**, 305.

MIED, R. P. 1976 The occurrence of parametric instabilities in finite-amplitude internal gravity waves. *J. Fluid Mech.* **78**, 763.

NOBLE, B. 1969 *Applied Linear Algebra.* Prentice-Hall.

PLUMB, R. A. 1977 The stability of small amplitude Rossby waves in a channel. *J. Fluid Mech.* **80**, 705.

RHINES, P. B. 1975 Waves and turbulence on a beta-plane. *J. Fluid Mech.* **69**, 417.